MET O 11 TECHNICAL NOTE NO.148

A variable reference atmosphere for the meso-scale model

BY

M.P. Kissane

MET O 11
Forecasting Research Branch
Meteorological Office
London Road
Bracknell, Berks

FH2A

A VARIABLE REFERENCE ATMOSPHERE FOR THE MESO-SCALE MODEL

Introduction

The current formulation of the meso-scale model (Tapp and White, 1976; Carpenter, 1979) uses the Exner function, Π, and potential temperature, Θ, as model variables. These are defined by

$$\Pi = \left(\frac{\rho}{\rho_s}\right)^{R/c_p} \quad \text{and} \quad \Theta = \frac{p_s}{\rho R}\left(\frac{c_p}{R} - 1\right)\Pi$$

where p_s is a basic pressure constant. Potential temperature is expanded in terms of a constant reference value, Θ_0, plus a perturbation, Θ_1. This reference value is used via a hydrostatic relationship to determine a vertically varying reference pressure*, ρ_0. So we have

$$\Theta = \Theta_0 \text{ (constant)} + \Theta_1(\underline{r}, t) \tag{1}$$

$$\Pi = \rho_0(z) + \rho_1(\underline{r}, t) \tag{2}$$

where z is height above mean sea level.

The modification described here allows Θ_0 to depend on height. This change is desirable since it can reduce the magnitude of perturbations Θ_1 and ρ_1 away from the reference state. This should, in particular, promote greater accuracy in the model's floating point calculation of derivatives of Θ_1 and ρ_1 especially over orography and when the model is deep. A more important effect of the modified reference state may be the improvement of the representation of the atmosphere's vertical modes in the Helmholtz operator of equation (17). This will make the numerical solution to the Helmholtz equation closer to the true solution which also aids the stability of the semi-implicit numerical scheme.

The vertical co-ordinate of the model, η, is height above orography given by

$$\eta = z - E(x, y) \tag{3}$$

*As no ambiguity exists from her on the Exner function will be referred to as pressure.

Initially the new reference atmosphere was viewed merely as a device to achieve the benefits described above, the only constraint being that it was separable into a sum of orographic and η-dependent terms. The consequence of not satisying this is the extra complexity (and hence computation) that results when the time differencing is performed and it is required to vertically decouple the Helmholtz equation formed in section 3. That approach was abandoned because it allowed reference atmospheres that were not consistent with a state of no motion. Forms of Θ_0 and P_0 could be used which subtracted some potential motion from the initial fields this being reintroduced after integration of the model in forming the final fields. Clearly this adversely affected the evolution of the forecast although the effects were far from obvious in early runs of this version of the model. The reference atmosphere used subsequently was a function of z and static.

2. The reference atmosphere

Pressure and potential temperature are expanded as

$$P = P_0(z) + P_1(\underline{r}, t) \tag{4}$$

$$\Theta = \Theta_0(z) + \Theta_1(\underline{r}, t) \tag{5}$$

where P_0 is determined by the choice of Θ_0 through the hydrostatic relationship

$$\frac{dP_0}{dz} = -\frac{g}{c_p \Theta_0} \tag{6}$$

with boundary condition $P_0(0) = 1$. In general Θ_0 would be non-linear. However, because of the vertical co-ordinate used (equation (3)), and reasons given in the introduction, Θ_0 must have a linear dependence on z. Then we can write

$$\Theta_0(z) = az + b \equiv \Theta_0(\eta) + aE \tag{7}$$

where, for example, a and b are determined by average values of potential temperature from the top and bottom of the model's initial fields. Equations

(7) and (5) give

$$P_o(z) = 1 - \frac{g}{ac_p} \ln\left(\frac{a}{b} z + 1\right)$$

$$\equiv P_o(\eta) - \frac{g}{ac_p} \ln\left(\frac{aE}{a\eta + b} + 1\right) \qquad (8)$$

This is not entirely satisfactory since the orographic term depends on η but is the best that can be achieved. This inseparability of $P_o(z)$ is not serious but does lead to extra computation. The difference of this reference pressure from that resulting from a constant Θ_o can be seen by expanding equation (8) to third order in z

$$P_o(z) \simeq 1 - \frac{g}{c_p b}\left(z - \frac{a}{2b} z^2 + \frac{a^2}{3b^2} z^3 \ldots\right) \qquad (9)$$

where originally

$$P_o(z) = 1 - \frac{g}{c_p \Theta_o} z \qquad (10)$$

3. The equations of the model

The three equations of motion, the continuity equation and the heat equation become respectively

$$\frac{Du}{Dt} = fv - c_p \textcircled{H}\left(\frac{\partial P_1}{\partial x} - \frac{\partial E}{\partial x}\frac{\partial P_1}{\partial \eta}\right) = X \qquad (11)$$

$$\frac{Dv}{Dt} = -fu - c_p \textcircled{H}\left(\frac{\partial P_1}{\partial y} - \frac{\partial E}{\partial y}\frac{\partial P_1}{\partial \eta}\right) = Y \qquad (12)$$

$$\frac{D\dot{\eta}}{Dt} = \frac{g\Theta_1}{\Theta_o(\eta+E)} - c_p \textcircled{H}\frac{\partial P_1}{\partial \eta} - \frac{D}{Dt}\left(u\frac{\partial E}{\partial x} + v\frac{\partial E}{\partial y}\right) \qquad (13)$$

$$\frac{DP_1}{Dt} = \frac{g}{c_p \Theta_o(\eta+E)}\left(\dot{\eta} + u\frac{\partial E}{\partial x} + v\frac{\partial E}{\partial y}\right) + (\gamma - 1)\frac{\mathbb{P}}{\textcircled{H}}\frac{D\Theta}{Dt} - (\gamma - 1)\mathbb{P}\,\underline{\nabla}\cdot\underline{v} \qquad (14)$$

$$\frac{D\textcircled{H}}{Dt}\left\{= \frac{D\Theta_1}{Dt} + \underline{v}\cdot\underline{\nabla}\Theta_o(\eta+E)\right\} = \frac{Q}{c_p \mathbb{P}} \qquad (15)$$

where Q is the diabatic heating and $\dot{\eta} = \frac{\partial \eta}{\partial t}$

It should be mentioned that the minor simplifications performed on the fundamental continuous equations of motion to obtain equations (11), (12) and (13) cannot be performed on the fundamental equations once spatially discretized (according to the model's differencing scheme). That is the spatially discretized verions of equations (11), (12) and (13) are somewhat artificial because they do not follow from the discretized fundamental equations. However, a differencing scheme that facilitates manipulations consistent with the required continuous equation manipulation is unlikely to produce anything more than very minor changes in the forecast and no attempt was made here towards consistency.

The time differencing of the model treats implicitly those terms involving sound wave propogation in a flat adiabatic atmosphere. All others (including those arising from the change in reference atmosphere) are used at time levels (n) or (n-1) as desired for numerical stability. The time-discretized forms of equations (11), (12); (13) and (14) are then used to eliminate $u^{(n+1)}$, $v^{(n+1)}$ and $\dot{\eta}^{(n+1)}$ from equation (14). In this way a Helmholtz equation is derived for the second order pressure function π where

$$\pi = c_p \left(\mathbb{P}^{(n+1)} - 2\mathbb{P}^{(n)} + \mathbb{P}^{(n-1)} \right) \tag{16}$$

giving

$$\nabla^2 \pi + \left\{ \frac{\partial^2}{\partial \eta^2} + \left(\frac{a}{\theta_0(\eta)} - \frac{g}{c_0^2} \right) \frac{\partial}{\partial \eta} - \frac{1}{c_0^2 \delta t^2} \right\} \pi = R \tag{17}$$

with equation (15) giving

$$\theta_i^{(n+1)} = \theta_i^{(n-1)} - 2\delta t \left\{ \underline{v}^{(n)} \cdot \underline{\nabla} \theta_i^{(n)} + \frac{Q}{c_p \mathbb{P}} - a \left(\dot{\eta}^{(n)} + u^{(n)} \frac{\partial \bar{E}}{\partial x} + v^{(n)} \frac{\partial \bar{E}}{\partial y} \right) \right\} \tag{18}$$

where the speed of sound in the reference atmosphere $c_0(\eta) = (\gamma R P_0 \theta_0)^{1/2}$, δt is the timestep used and R is given in appendix A.

4. Results

The Hampstead storm case study (Bailey et al, 1980) was used to test the variable reference atmosphere version (v.r.a.v) of the model. The initial data is for 0600Z of the 14/8/75 with the model producing a forecast for 1800Z after 720 timesteps (i.e. δt = 1 minute). The values of $\Theta_o(z)$ used were 294K at $z = 0$ and 312K at z = 4 km (the top level of the model) giving a = 0.0045 Km^{-1}
and b = 294 K
The standard model used Θ_o = 300 K.

Charts in appendix B compare MSLP, potential temperature, horizontal wind vectors, vertical wind speeds, and vertical cross sections of potential temperature and wind vectors. The v.r.a.v of the model used 8% more C.P.U. time in producing the forecast on the IBM 360/195.

5. Discussion and conclusion

The v.r.a.v has produced an average half millibar reduction in pressure over the whole forecast area with very little change in pattern. This is a small improvement because the pressure is too high (by somewhat more than half a millibar!) in this case study as no control is asserted on the total flow in, or out, of the modelled volume. It can be seen from figure 4 and the vertical cross sections that vertical velocities are slightly reduced. The most obvious effect, however, concerns potential temperature. The air in the v.r.a.v. is generally cooler near the surface except over land unaffected by cloud (i.e. eastern England). This difference is most marked in the north west corner where it is > 2K at the surface and increases the static stability up to a height of 200 m relative to the standard forecast. The cause of this difference in north-west and the west seems, from grid point values not shown here, to be due to a small but persistent increase in westerly inflow relative to the standard version.

This experiment indicates that the use of the variable reference atmosphere does give a very similar forecast but the possible importance of the differences in predicted weather justifies the extra computation involved - further comparisons should decide this.

Acknowledgements

My thanks to Dr. K.M. Carpenter for useful discussion during this work and to Dr P.W. White and Mr M.J. Dutton for commenting on the first draft of this note.

References

Bailey, M.J., Carpenter, K.M., Lowther, L.R., Passant, C.W., 1980 'A mesoscale forecast for 14 August 1975 - the Hampstead storm'. Met O 11 T.N. no. 143

Carpenter, K.M., 1979, 'An experimental forecast using a non-hydrostatic meso-scale model', Q.J.R. Met. Soc. 105, 629-655.

Tapp, M.C., White, P.W., 1976, 'A non-hydrostatic meso-scale model' Q.J.R. Met. Soc. 102, 277-296.

Appendix A

$$R = \frac{2}{c_0^2 \delta t}\left\{ c_p \underline{v}^{(n)} \cdot \underline{\nabla} p_1^{(n)} - \frac{g}{\theta_0(z)}\left(u^{(n)} \frac{\partial E}{\partial x} + v^{(n)} \frac{\partial E}{\partial y} \right) \right.$$

$$+ \frac{g}{\theta_0(\eta)}\left(\frac{\alpha E}{\theta_0(z)} \dot{\eta}^{(n)} - \dot{\eta}^{(n-1)} \right) + \gamma R \left(p_1^{(n)} - \frac{g}{\alpha c_p} \ln\left[\frac{\theta_0(z)}{\theta_0(\eta)} \right] \right) \underline{\nabla} \cdot \underline{v}^{(n)}$$

$$\left. - \gamma R \frac{\mathbb{P}^{(n-1)}}{\Theta^{(n-1)}} \frac{D\Theta}{Dt} + \gamma R p_0(\eta) \underline{\nabla} \cdot \underline{v}^{(n-1)} \right\}$$

$$+ \frac{2 c_p}{c_0^2 \delta t^2}\left(p_1^{(n)} - p_1^{(n-1)} \right) + \frac{1}{\theta_0(\eta) \delta t}\left(\frac{\partial X}{\partial x} + \frac{\partial Y}{\partial y} + \frac{\partial H}{\partial \eta} - \frac{g}{c_0^2} H \right)$$

where

$$X = -2\delta t \left\{ \underline{v}^{(n)} \cdot \underline{\nabla} u^{(n)} - f v^{(n)} + c_p \Theta^{(n)} \left(\frac{\partial p_1}{\partial x} - \frac{\partial E}{\partial x} \frac{\partial p_1}{\partial \eta} \right) - F_x \right\}$$

$$Y = -2\delta t \left\{ \underline{v}^{(n)} \cdot \underline{\nabla} v^{(n)} + f u^{(n)} + c_p \Theta^{(n)} \left(\frac{\partial p_1}{\partial y} - \frac{\partial E}{\partial y} \frac{\partial p_1}{\partial \eta} \right) - F_y \right\}$$

$$H = -2\delta t \left\{ \underline{v}^{(n)} \cdot \underline{\nabla} \dot{\eta}^{(n)} - g \frac{\theta_1}{\theta_0(z)} + c_p \Theta^{(n)} \frac{\partial p_1}{\partial \eta} - F_\eta \right.$$

$$\left. + \frac{\partial E}{\partial x} X + \frac{\partial E}{\partial y} Y + u^{(n)2} \frac{\partial^2 E}{\partial x^2} + 2 u^{(n)} v^{(n)} \frac{\partial^2 E}{\partial x \partial y} + v^{(n)2} \frac{\partial^2 E}{\partial y^2} \right\}$$

where $\underline{F}$ represents friction, diffusion and numerical smoothing and X and Y are given by equations (11) and (12).

Appendix B

The forecast region with the positions of Hampstead and the vertical cross sections is shown below

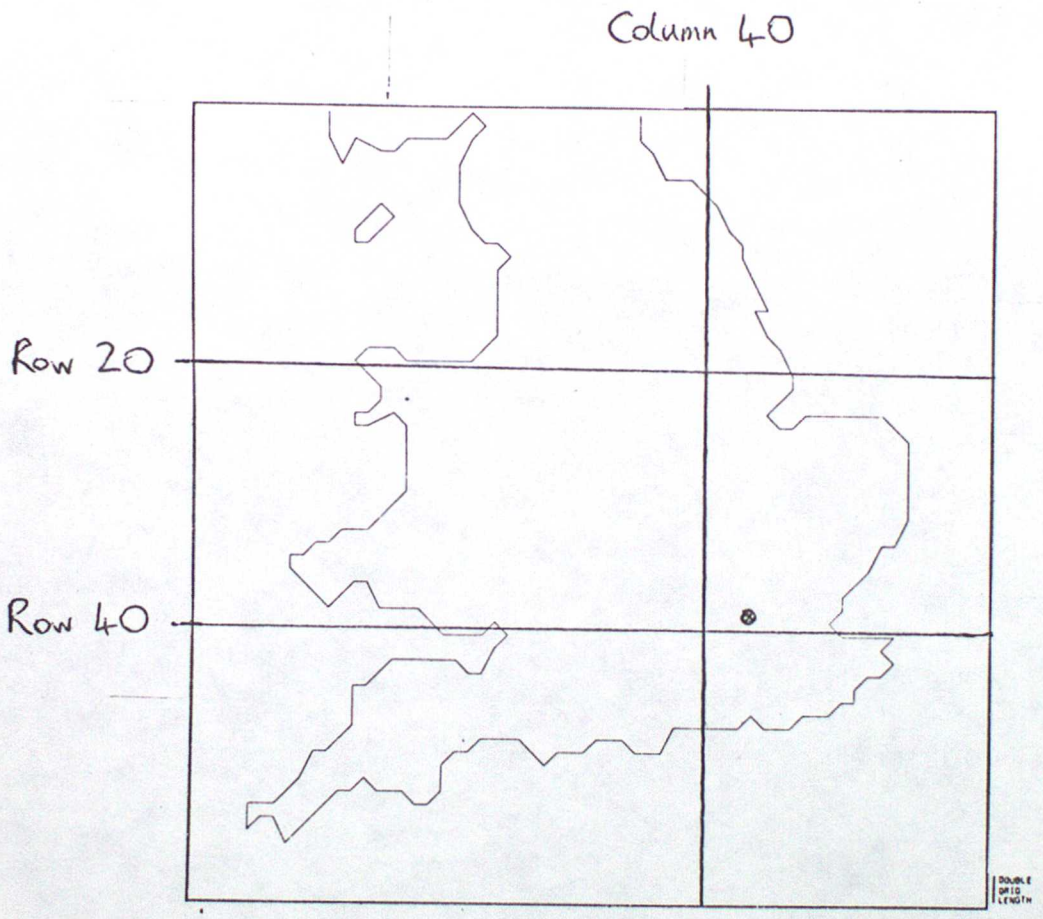

In the following figures "a)" refers to the standard model's forecast while "b)" refers to the new version's forecast

Figure 1

Mean sea level pressure
Isobar interval .5 mb

a)

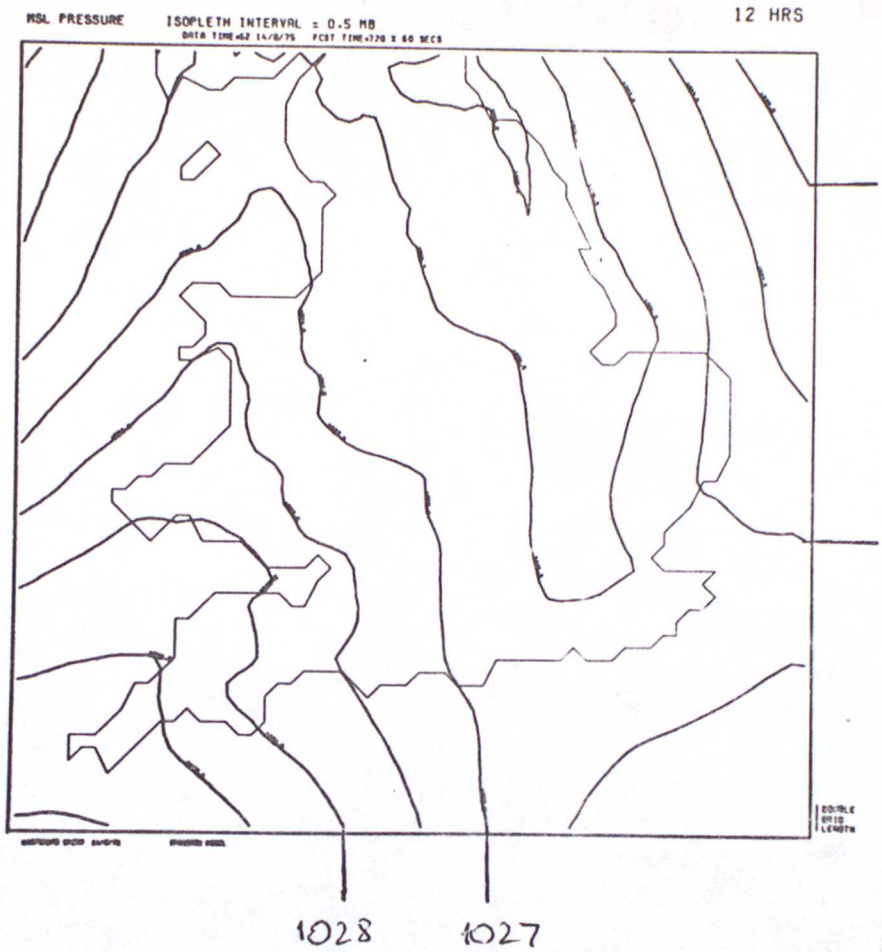

b)

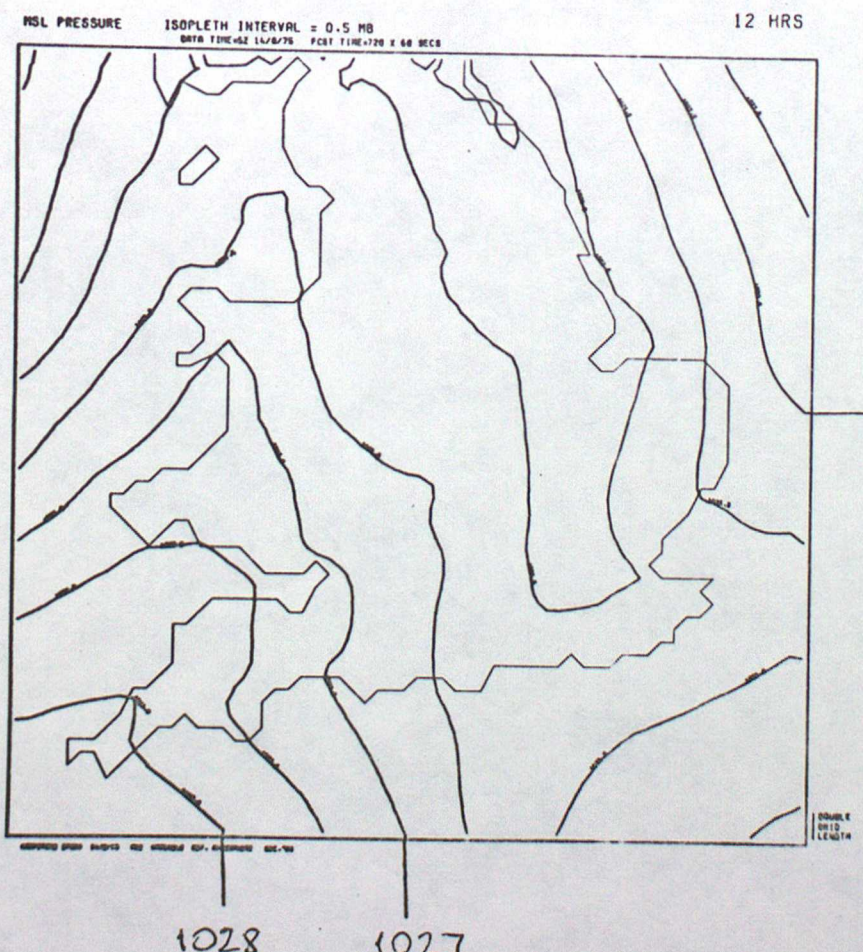

Figure 2

Potential temperature at 10m above surface. Isotherm interval 1°C

a)

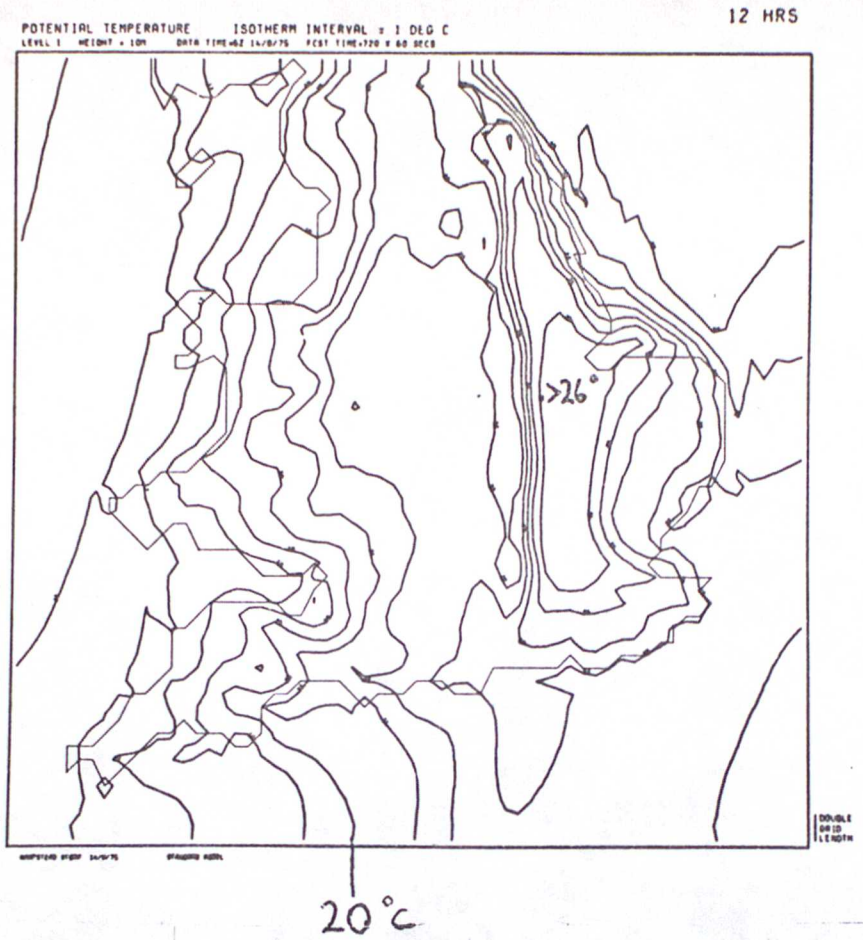

b)

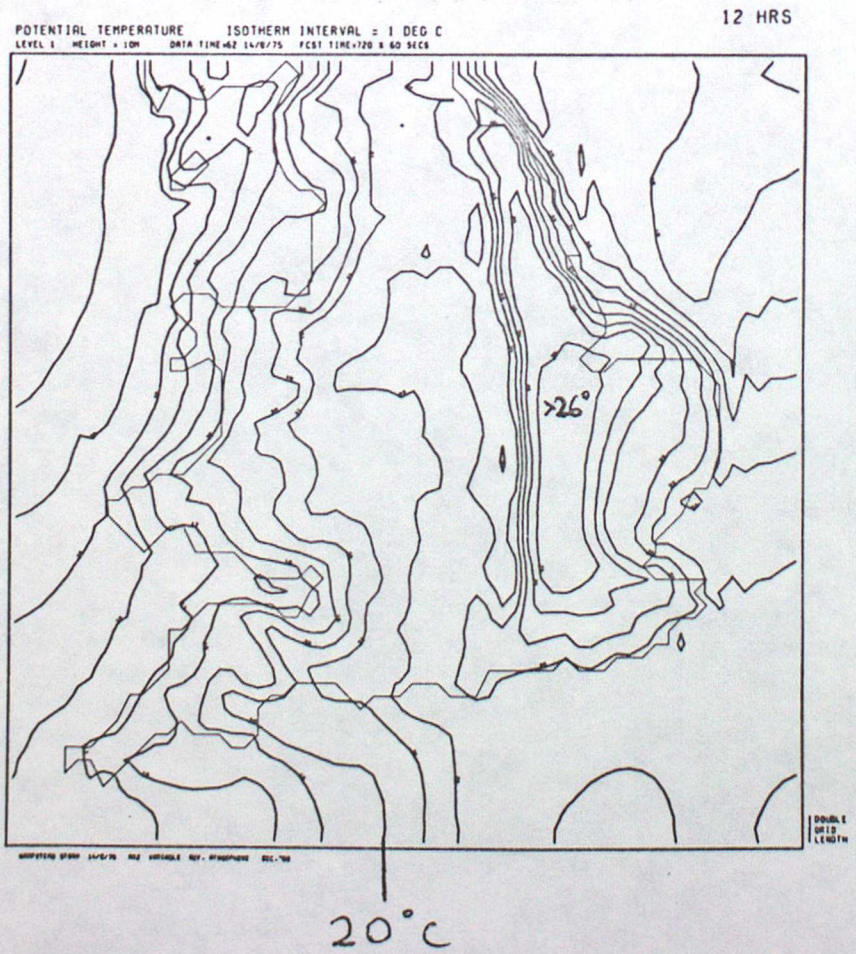

Figure 3

Wind vectors at 10m above surface

a)

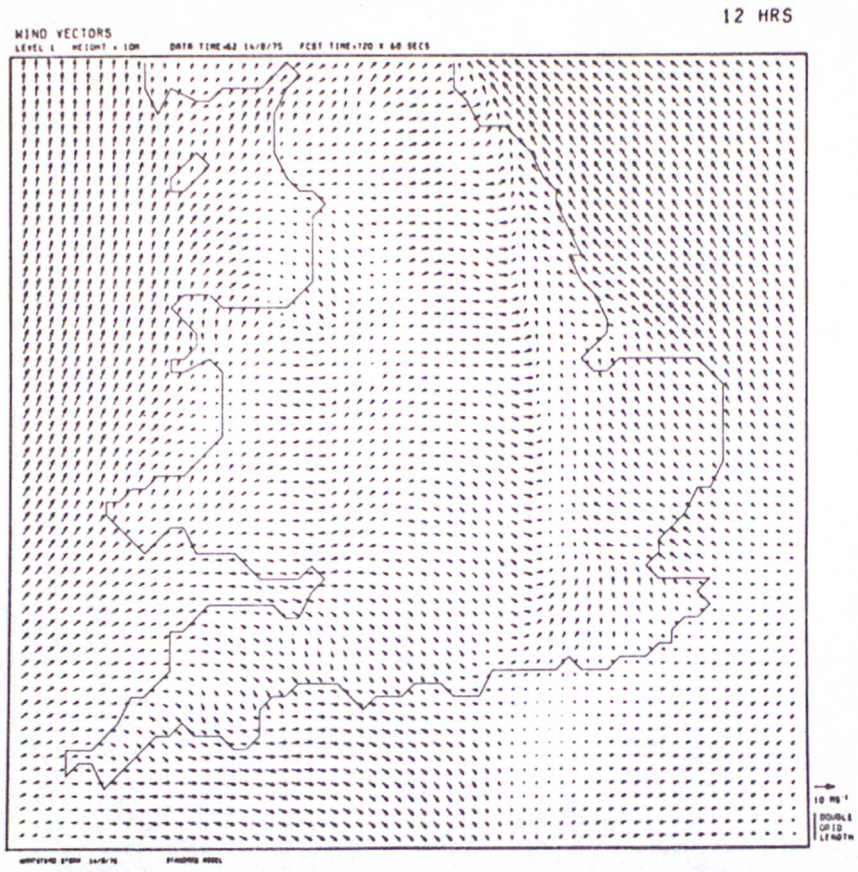

b)

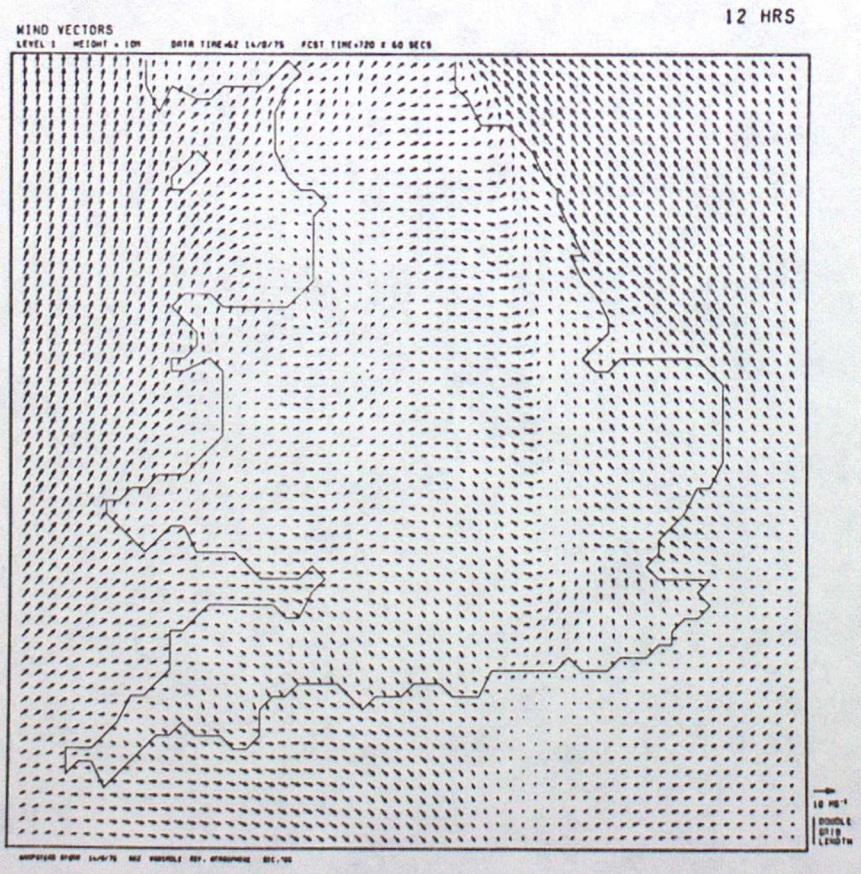

Figure 4

Vertical velocity at 190m above surface. Isopleth interval 8 cm s^{-1}

a)

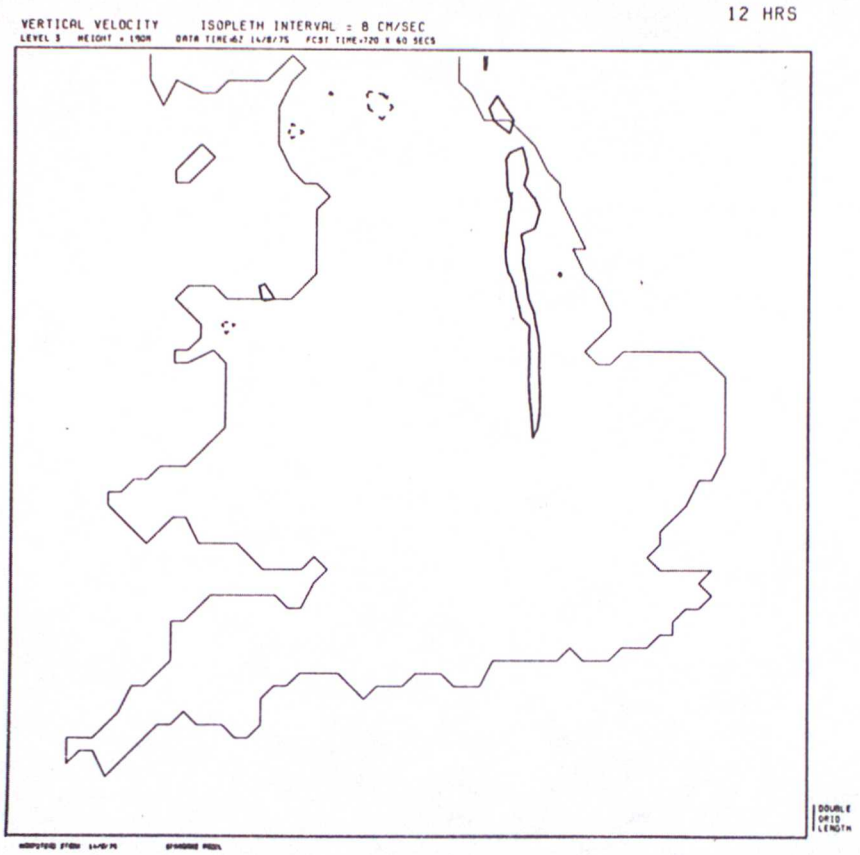

b)

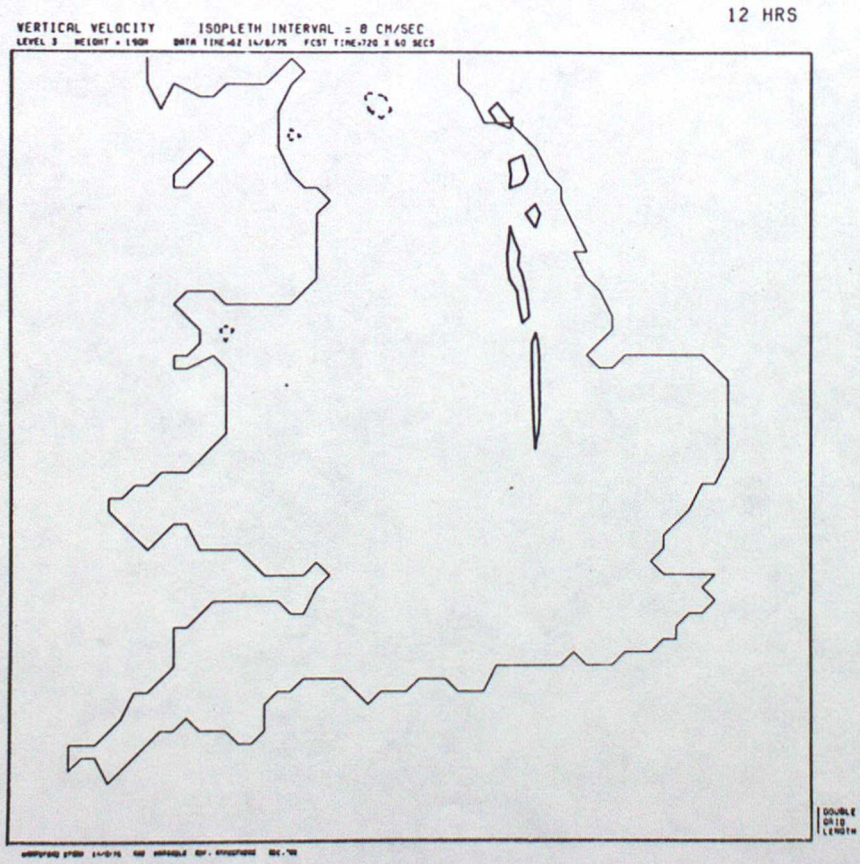

Figure 5

Wind vectors and potential temperature along column 40.
Isotherm interval 1°C

a)

12 HRS

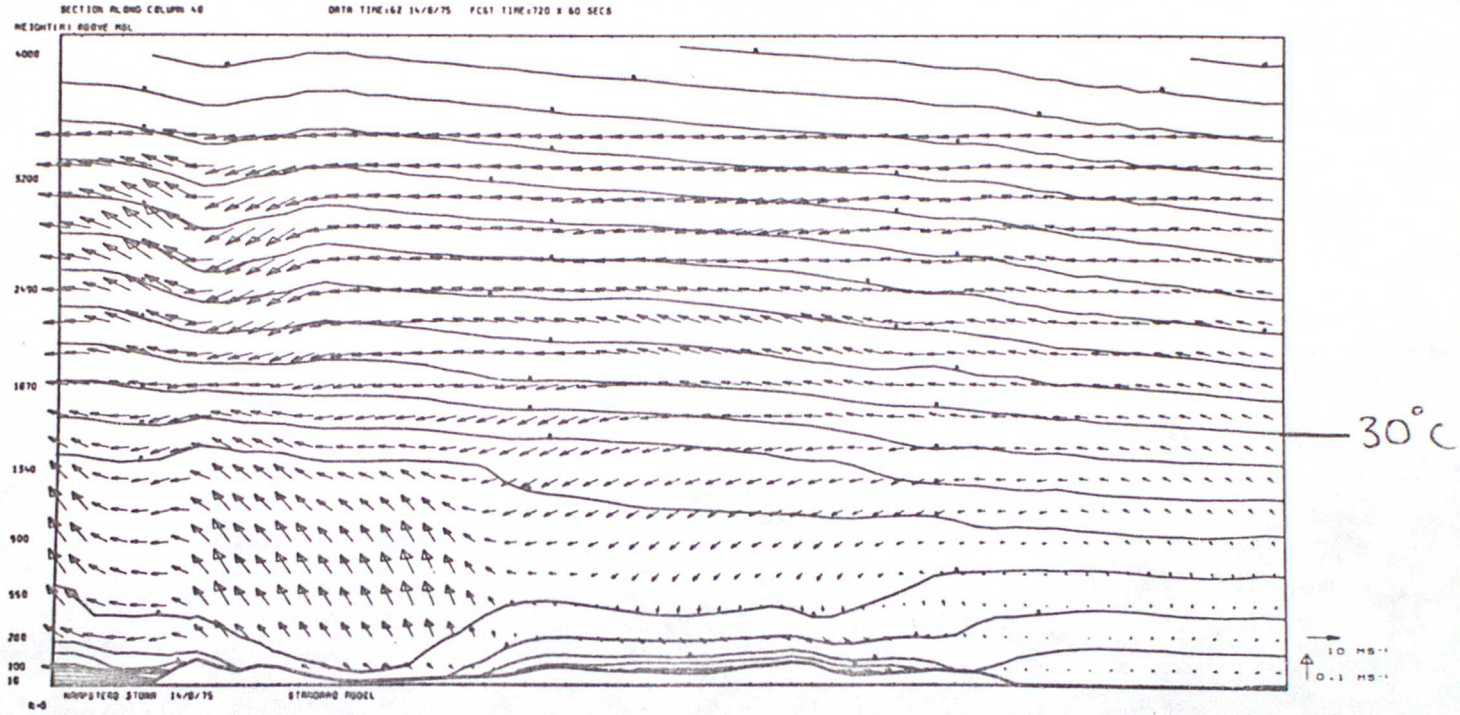

b)

12 HRS

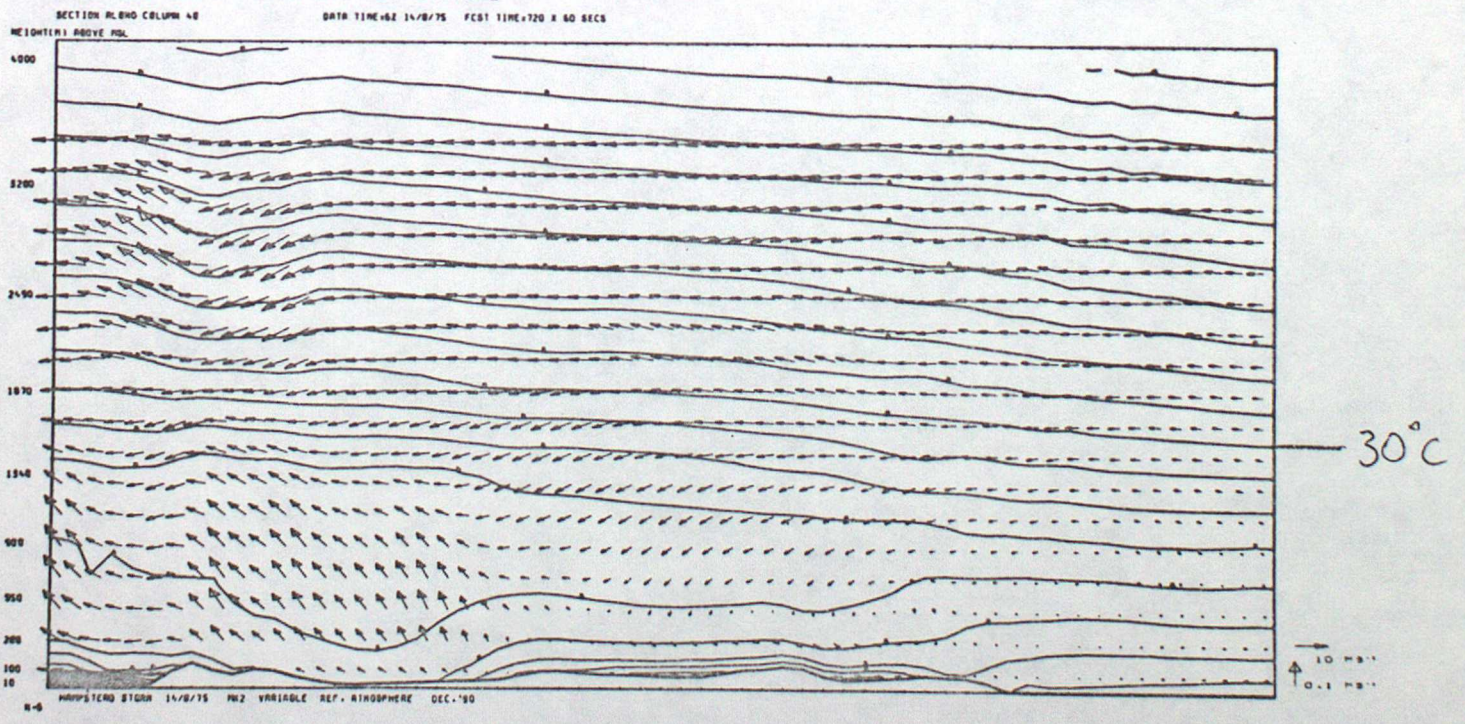

Figure 6

Wind vectors and potential temperature along row 20.

Isotherm interval 1°c

12 HRS

a)

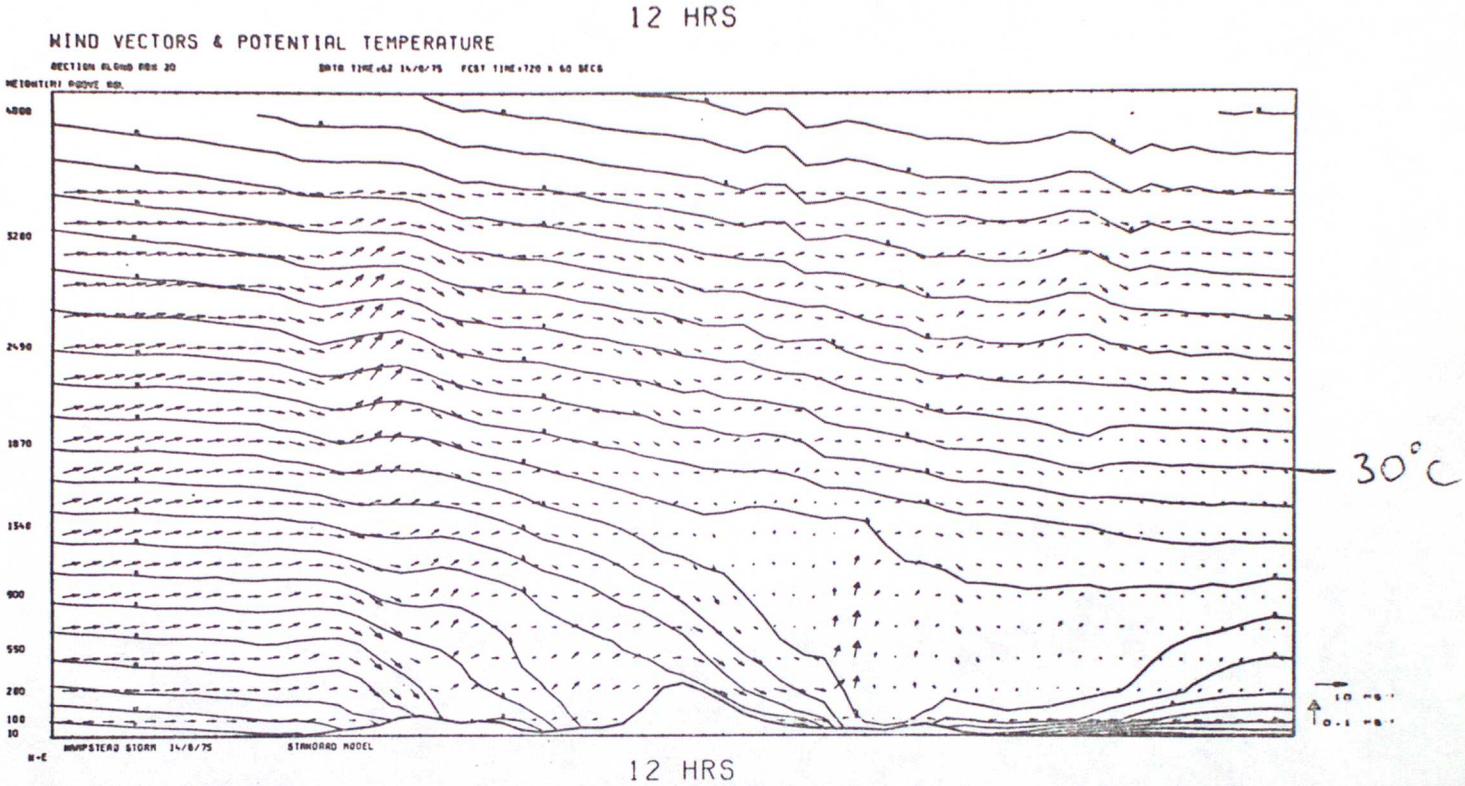

12 HRS

12 HRS

b)

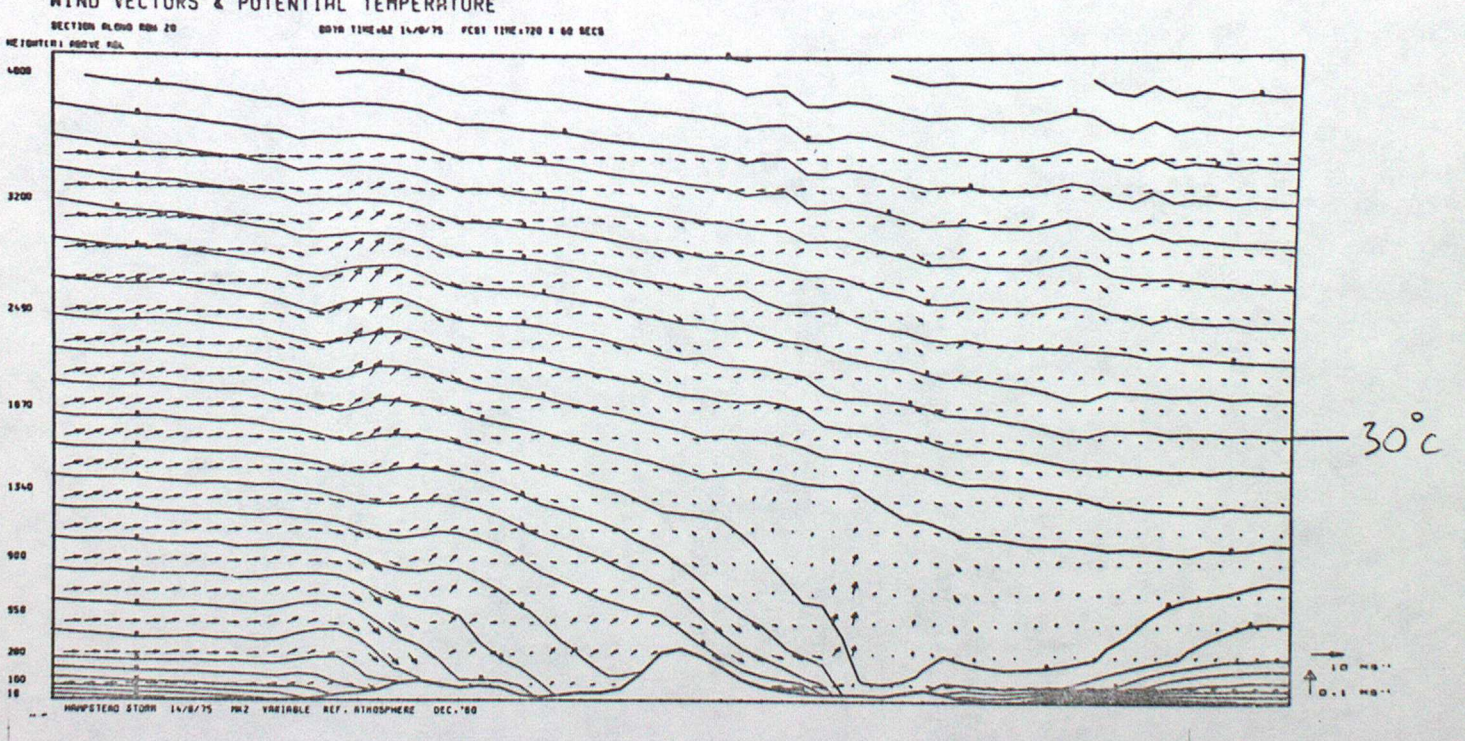

Figure 7

Wind vectors and potential temperature along row 40.

Isotherm interval 1°C

12 HRS

a)

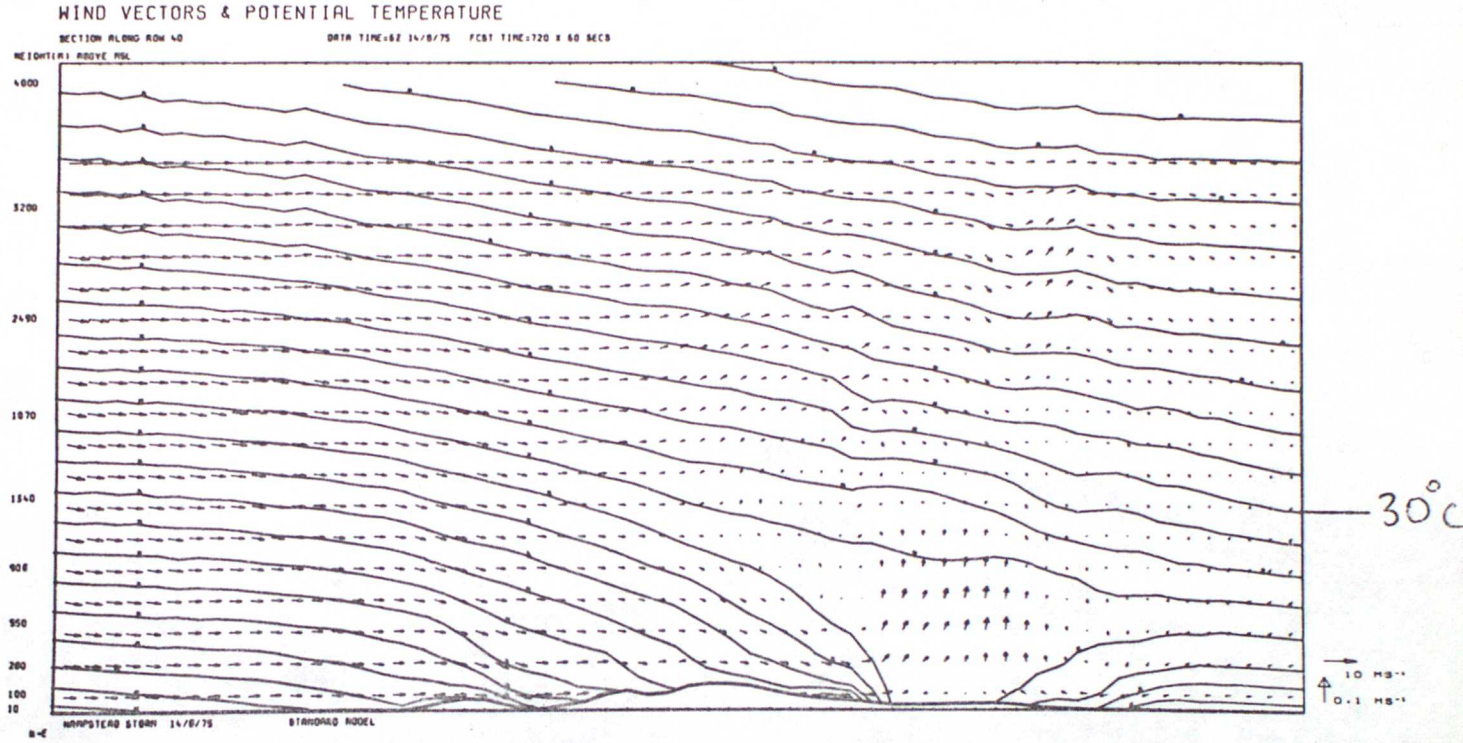

12 HRS

b)